U.S. DEPARTMENT OF THE INTERIOR

U.S. GEOLOGICAL SURVEY

High-Precision Temperature Logging at GISP2, Greenland, May 1992

by

Gary D. Clow[1], Richard W. Saltus[2], and Edwin D. Waddington[3]

Open-File Report 95-490

1995

[1]U.S. Geological Survey, Menlo Park, California
[2]U.S. Geological Survey, Denver, Colorado
[3]University of Washington, Seattle, Washington

Abstract

We describe a logging system capable of making high-precision temperature measurements and present an analysis of the measurement errors. This system was used to acquire a continuous temperature log in the GISP2 icecore hole just before drilling operations began for the 1992 field season. The system's sensitivity was 0.14 mK (0.00014°C) during this log. The precision of the processed data is 0.7 mK and the accuracy is 4.5 mK. Temperature gradients were found to slightly exceed the theoretical gradient required for the onset of natural convection of the borehole fluid (n-butyl acetate) in a narrow zone between 210 and 330 m. However, a monitoring experiment failed to detect evidence for convection at these depths. At the time of the 1992 log, temperatures in and around most of the borehole are predicted to have still been perturbed by 0.4–1.0 mK due to the previous year's drilling activities; within a couple hundred meters of the surface, the disturbance is predicted to have been much larger ($\sim$ 10 mK). If the near-surface drilling disturbance was in fact still this large during May 1992, it will take at least 7 additional years for the near-surface disturbance to dissipate to a level commensurate with the precision of the logging system, i.e. $\sim$ 1 mK.

Introduction

The subsurface temperature transients resulting from temperature changes on the earth's surface during the last $\sim$ 40 ka are still stored within the ice sheet at Summit, Greenland. The two deep boreholes recently completed at this site provide an ideal setting in which to *directly measure* these climatically-induced temperature transients. Once borehole temperature (BT) measurements have been made, the surface-temperature history for Summit can be reconstructed using appropriate geophysical inversion techniques. This method provides a means for assessing past climatic changes that is completely independent of the stable isotope proxies.

Unfortunately, any surface-temperature history derived from a set of borehole temperature measurements will be "smeared" in time. This is primarily a consequence of the heat diffusion process. While it cannot be eliminated, the effect of this temporal smearing on reconstructed surface temperatures can be minimized through optimal experimental design. Application of the Backus-Gilbert inverse methods to the BT-inverse problem demonstrates that our ability to *resolve* past climatic events can be optimized by reducing the random errors in the temperature measurements to 1 mK, or better (*Clow*, 1992). This is illustrated in Figure 1. In this figure, the high-frequency line represents a hypothetical surface-temperature history from which synthetic borehole temperatures have been calculated. The bold smooth line is the surface-temperature history reconstructed from the synthetic BT data for various levels of random noise. The improvement obtained by reducing the uncertainty in the temperature measurements from 10 to 1 mK is quite apparent.

Based on these results, the U.S. Geological Survey's portable temperature logging system was modified to further reduce instrumental sources of measurement error. Our objective was to build a system capable of making borehole temperature measurements in remote polar regions with a precision better than 1 mK and an accuracy of at least 5 mK. In this paper, we will: 1) describe the modified logging system and the associated measurement errors, 2) describe the temperature log acquired in the GISP2 borehole during May 1992, using this system, and 3) discuss the thermal disturbances that affect the temperature measurements made in the GISP2 borehole, i.e. disturbances associated with the drilling process and with fluid convection within the borehole.

USGS Temperature Logging System

Several techniques are currently used for measuring temperatures in boreholes (see *Beck and Balling*, 1988). Most commonly, the resistance of a temperature sensor (thermistor or RTD) is determined by measuring the voltage drop across the sensor when passing an excitation current through it. This function is provided either by a commercial digital multimeter (DMM) or by a custom-built electronic bridge. An advantage of custom circuitry is that it can be made small enough to be included in an instrument package located at the downhole end of the logging cable, keeping the lead lengths to the sensor relatively short. This package can be designed to measure several other parameters as well, such as fluid pressure and borehole diameter, and the resulting data can be temporarily stored within the instrument package or multiplexed to the surface through

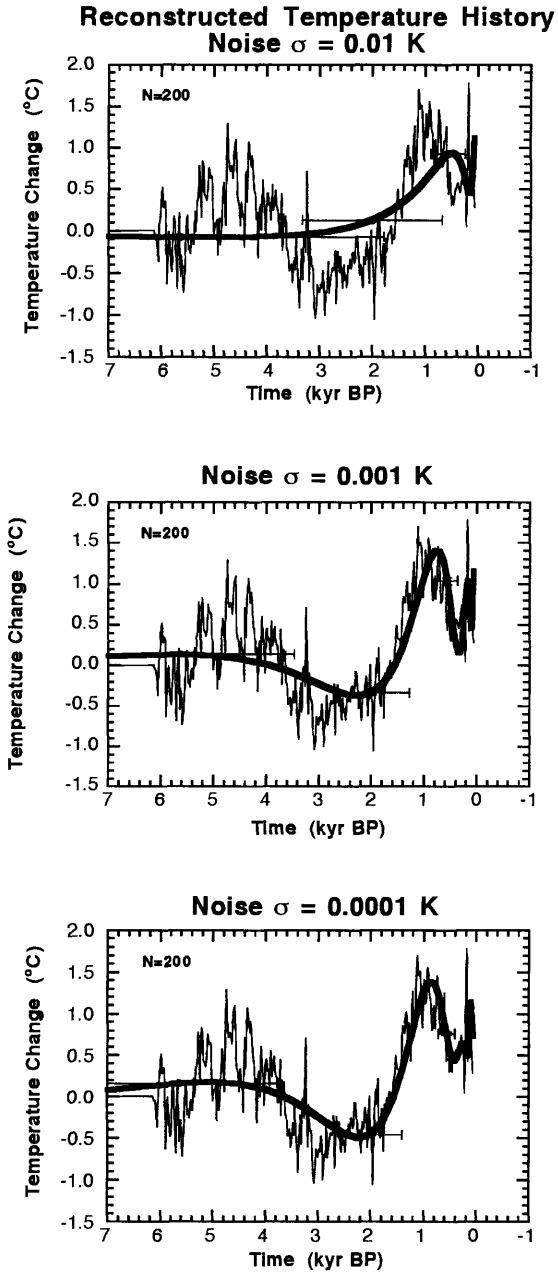

Figure 1: Temperature histories (bold lines) reconstructed from noisy synthetic borehole data. Noise levels are 10 mK, 1 mK, and 0.1 mK. The high-frequency line in each panel represents a hypothetical surface-temperature history used to calculate the synthetic borehole data. The mismatch between the hypothetical history and the reconstructed histories indicates the extent of the "temporal smearing" in the solutions; this is also indicated by the length of the horizontal lines at 560, 2000, and 5600 years BP. A significant increase in resolving power is obtained by reducing the random errors in the borehole temperatures to the 1 mK level. 200 data points were used in these reconstructions.

a cable with just a couple of conductors. A significant disadvantage of this approach for borehole temperature measurements is that it is very difficult to maintain the calibration of the resistance measuring circuit since the temperature of the instrument package will often change by 10–30 K during a logging experiment. This can cause errors of 10 mK, or more, in the resulting temperature measurements. Although the use of a commercial digital multimeter on the surface potentially requires very long lead lengths, the DMM can be maintained at a constant temperature, eliminating temperature-related drift in the measuring circuit. In addition, the DMM's calibration can be periodically rechecked while the measurements are in progress. With some systems, temperature measurements can be made while driving the sensor downhole at a constant speed ("continuous" logging), while with others, measurements can only be made when the probe is stopped at a fixed depth. The latter method, known as "incremental" or "stop-and-go" logging, results in a limited number of measurements at fixed depths. However, these measurements are free of the "slip-ring" noise (discussed later) inherent in continuous temperature logs. In addition, equilibrium temperatures can be directly measured using the incremental mode, eliminating the need to deconvolve the measured signal to account for the finite response time of the probe. Depths are normally determined by measuring the rotation of a calibrated cable pulley using an optical encoder and/or by measuring the pressure near the temperature sensor as the probe descends.

The U.S. Geological Survey's PCR logging system[1] utilizes a commercial DMM that resides on the surface in a temperature-controlled box. This strategy was adopted to allow the logging of boreholes with diameters as small as 2.5 cm and to minimize the temperature drift in the measuring circuit. The resistance of the temperature sensor is determined using a 4-wire resistance measurement that compensates for the resistance of the 4-conductor logging cable (Fig. 2). A "slip-ring" assembly provides electrical continuity between the logging cable (mounted on a rotating drum) and the multimeter. Measurements can be made in either the continuous or incremental logging modes. Depth information is provided solely by an optical encoder mounted on a calibrated cable pulley; the inclusion of a pressure transducer in the system, although desirable, would require additional conductors in the logging cable. The system is controlled by a laptop computer which displays and stores the resistance, depth, time, and logging speed. Resistance is converted to temperature during the data processing step.

The characteristics of this type of system are as follows: 1) The temperature sensitivity is given by the ratio of the smallest resistance ΔR resolvable by the multimeter to the change in probe resistance per degree change in temperature ($\partial R_s/\partial T$). Because of their high sensitivity and ruggedness, we use negative-temperature-coefficient (NTC) thermistor probes exclusively with the PCR system. With this type of sensor, the probe's sensitivity can be described by $(\partial R_s/\partial T) \approx \alpha_T R_s$, where α_T is the probe's "temperature coefficient" (α_T is -0.04 to -0.07 K^{-1} for most commercially available NTC thermistors at the temperatures encountered in polar ice sheets). Thus, the system's temperature sensitivity is simply

$$\Delta T \approx \frac{\Delta R}{\alpha_T R_s}. \tag{1}$$

[1]The USGS has two primary temperature logging systems. The system described in this paper is the one used for polar climate research (PCR).

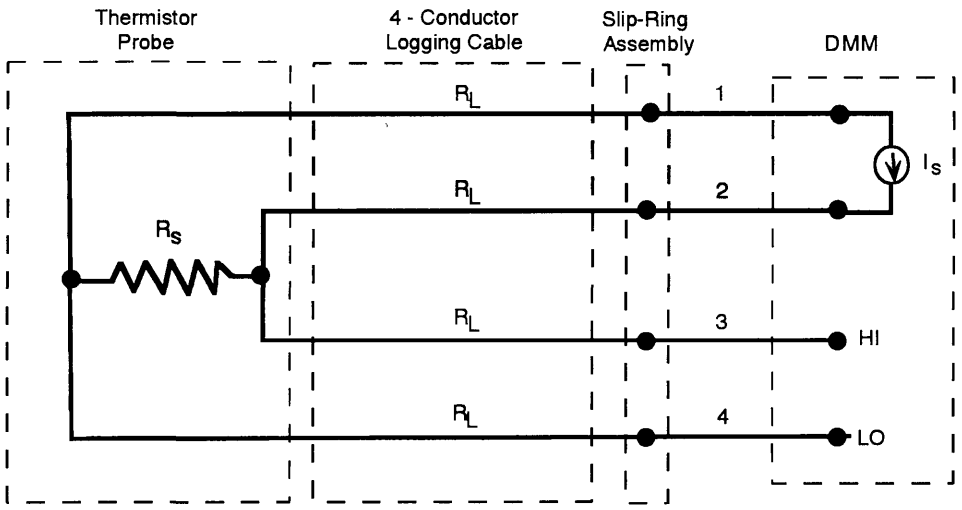

Figure 2: 4-wire resistance circuit utilized by the logging system. Leakage paths between the following conductor pairs will cause measurement errors ϵ_l: 1–2, 1–3, 2–4, 3–4.

The system's sensitivity can be enhanced by using a probe whose resistance at the temperature being measured is near the high end of one the resistance scales on the DMM.

2) Leakage paths between the conductors in the 4-wire circuit via the insulation can produce a large error in the resistance measurement. Examination of the circuit in Figure 2 reveals which paths will cause such an error. For the critical leakage paths, the error in the associated temperature measurement is

$$\epsilon_l \approx \frac{R_s}{\alpha_T(R_s + R_l)}, \tag{2}$$

where R_l is the resistance of the leakage path. Thus, R_s should be kept small to minimize the leakage error ϵ_l. However, an additional constraint is that R_s should be greater than the lead resistance R_L for each leg of the 4-wire circuit in order for an accurate resistance measurement to be made. As a rule of thumb, we find that R_s should be at least 10 times R_L.

3) As the source current I from the multimeter passes through the temperature sensor, the probe will warm above the ambient temperature by an amount

$$\epsilon_h = \frac{I^2 R_s}{\delta}, \tag{3}$$

where δ is the power dissipation constant which depends both on the probe design and on the thermal properties of the fluid in which the measurements are being made. This "self-heating" effect can be accounted for to a large extent during the data processing step since the current I and the probe resistance R_s are well-known. However, the correct value for the dissipation constant δ under field conditions is generally somewhat uncertain and so it is best to minimize the self-heating effect, if possible. The best strategy for doing

this is to use a multimeter which employs relatively small source currents and a probe specifically designed to reduce this effect.

4) Because the logging cable has a capacitance C, the 4-wire resistance circuit acts like a low-pass filter with a natural response time $\tau = R_s C$. Two issues arise here: A) In order to properly record the changing probe resistance, τ must be much less than the time scale for the resistance changes $[\tau \ll R_s(\partial R_s/\partial t)^{-1}]$. B) Assuming the condition in (A) is satisfied, small currents through the effective capacitance will still cause an error $\Delta R \approx \tau(\partial R_s/\partial t)$ in the resistance measurement. The associated error in temperature is

$$\epsilon_c = R_s C v \frac{\partial T}{\partial z}, \tag{4}$$

where v is the rate at which the probe descends into the borehole and $(\partial T/\partial z)$ is the local temperature gradient. The capacitance-related error ϵ_c can be minimized by keeping R_s and C relatively small, and by using a slow logging speed v.

From Equations 1–4 it is clear the temperature sensor plays a significant role in determining the characteristics of the overall system. The USGS's thermistor probes (design K212E, Fig. 3) are custom-made by Fenwal Electronics and consist of 20 small NTC bead thermistors divided into two packets, each of which is hermetically sealed in glass (*Sass et al.*, 1971). This prevents changes in the oxidation state of the metal oxide thermistors and relieves strain where the leads are attached to the ceramic body of the thermistors. As a result, the probes have excellent long-term stability; resistance drift is limited to 0.05% yr^{-1} or less (*Sass et al.*, 1971). The packets are wired in parallel so that only half of the multimeter's excitation current I passes through any given thermistor bead, reducing the self-heating effect. In addition, the thermistor packets are completely enclosed in a 4.0 mm diameter stainless steel shell to improve the ruggedness of the design; the probes can withstand the pressures encountered at 7–8 km in a fluid-filled borehole and the effects of hazardous chemicals such as n-butyl acetate. The use of many small thermistor beads, glass encapsulation, and a high-conductivity steel shell, all help to produce a high power-dissipation constant δ. The δ-value for the Fenwal K212E probes is 55 mW K^{-1} in circulating xylene and is believed to be similar when logging through n-butyl acetate. One disadvantage of these probes is their slow response time. We measured the time constant for a Fenwal K212E probe in butyl acetate while at GISP2 (*Saltus and Clow*, 1994) and found it to be 15.0 s, slow enough that a continuous temperature log must be deconvolved (*Saltus and Clow*, 1994) in order to recover the actual borehole temperatures even when the logging speed is relatively slow (e.g. 5 cm s^{-1}). The Fenwal K212E probes have a temperature coefficient α_T of about -0.055 K^{-1} at the temperatures encountered in the Greenland ice sheet.

For the 1992 temperature measurements, we used a 5.5-digit battery-powered DMM (Analogic DP100) that resolves 1Ω (0.1Ω) on the 200 kΩ (20 kΩ) scale using a 10μA excitation current. This multimeter integrates the input signal for 100 ms, eliminating line noise at frequencies beyond 10 Hz. A special slip-ring assembly was used to minimize the noise inherent in these electro-mechanical connectors. The 4.76 mm steel-armored logging cable contained 4 teflon-insulated conductors each of which had a resistance of 180 Ω. The capacitance of the 2200-m long cable was 0.35 μF. Although the optical encoder used with the PCR system can resolve depth changes of 2.5 mm, we only record depth to the nearest 2.5 cm for holes as deep as GISP2.

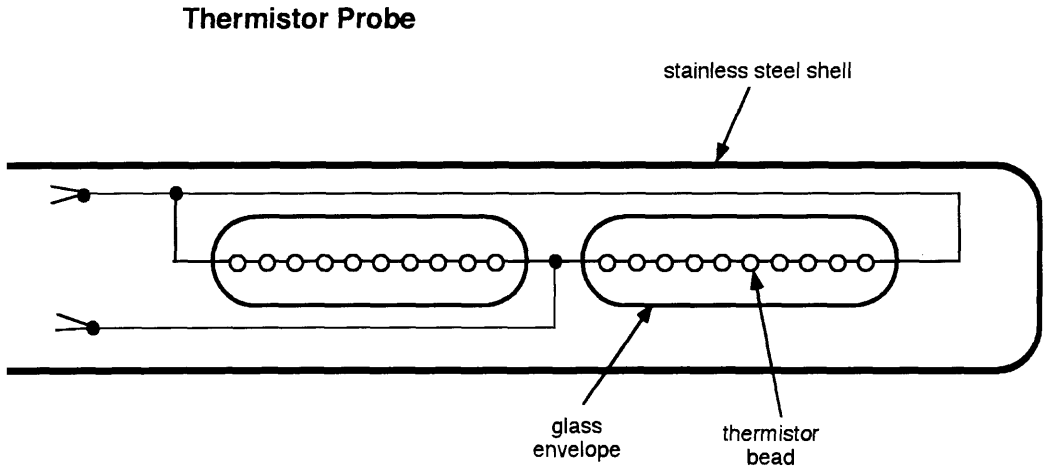

Figure 3: Fenwal K212E thermistor probe. The probe contains 20 small bead thermistors divided into two packets hermetically sealed in glass. The beads extend over a 9.57 cm length within a 4.0 mm diameter stainless steel shell.

Calibration Procedures

Both the temperature sensor and the logging system's multimeter require calibration. Probes are calibrated at the USGS in a copper equilibration block immersed in a temperature-controlled fluid bath (Hart model 7041) whose stability is estimated to be 0.5 mK. Block temperatures are established on the ITS-90 temperature scale by monitoring a NIST-calibrated Standard Platinum Resistance Thermometer (SPRT) with an 8.5-digit multimeter while the probe resistances are simultaneously measured with a 6.5-digit multimeter. For each sensor, approximately 100 (R_s, T) measurements are obtained at each of the calibration points, which are spaced every 5 K across the calibration range (−40°C to +30°C). The precision of the calibration data is estimated to be 0.2–0.3 mK while the accuracy is 4.5 mK, traced to the National Institute for Science and Technology (NIST). The (R_s, T) data are then used to establish the constants (a_i) in the 4-term calibration function

$$T^{-1} = a_0 + a_1(\ln R_s) + a_2(\ln R_s)^2 + a_3(\ln R_s)^3, \tag{5}$$

using weighted least squares. Applying an F-test (e.g. *Bevington*, 1969), we find that a much better fit can be obtained utilizing the 4-term function (Equation 5) instead of the often-used Steinhart-Hart Equation (*Steinhart and Hart*, 1968), particularly at cold temperatures. Figures 4 and 5 show the resulting calibration curve and the least-squares residuals for the probe (P1525) used to obtain the May 1992, temperature measurements at GISP2.

Before each logging run, the logging system's multimeter is brought up to its operating temperature (20–24°C) and allowed to stabilize for at least one hour. The DMM is then

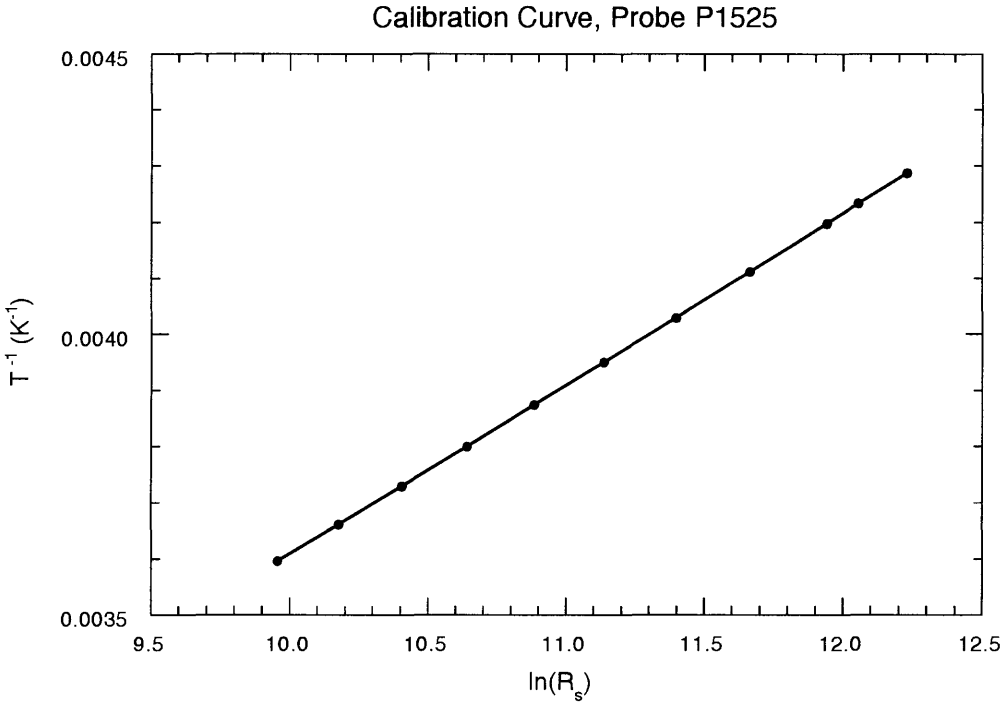

Figure 4: Calibration curve for probe P1525. Each calibration point represents an average about 100 (R_s, T) measurements. The averaging is done in $(\ln R_s, 1/T)$ space.

calibrated on site using a set of high-precision low-temperature-coefficient resistors that have also been maintained at 20–24°C for at least an hour. Errors in the multimeter's calibration constants result in an uncertainty of ≈ 0.15 mK in the subsequent temperature measurements. For deep boreholes such as GISP2, temperatures near the end of a logging experiment may be acquired up to 24 hours after the multimeter has been calibrated. During this time, the electronics of the multimeter can drift slightly. Based on the specifications of our present multimeter (Analogic DP100), this drift can cause an uncertainty of up to 0.67 mK during the course of a long logging run. In practise, we find our multimeter's 24-hour drift is about 1/4 of the quoted specification.

GISP2 Temperature Measurements

Just before drilling activities began for the 1992 field season, we obtained a temperature log (12 May) in the GISP2 borehole using the new logging system. The hole was then 1510-m deep and had been left undisturbed for 8.5 months. The DMM was field calibrated and then maintained at $20 - 24$°C for the duration of the logging experiment. For the bulk of the log, the resistance of the probe (P1525) was 123–132 kΩ, yielding a system sensitivity of 0.14 mK. All critical leakage paths were measured and found to have a resistance R_l exceeding 10 GΩ in all cases. Thus, the inter-conductor leakage error ϵ_l was less than 0.23 mK. The magnitude of the self-heating effect ϵ_h was also 0.23 mK. Despite the length of the logging cable, the response time of the circuit ($\tau \approx 45$ ms) was

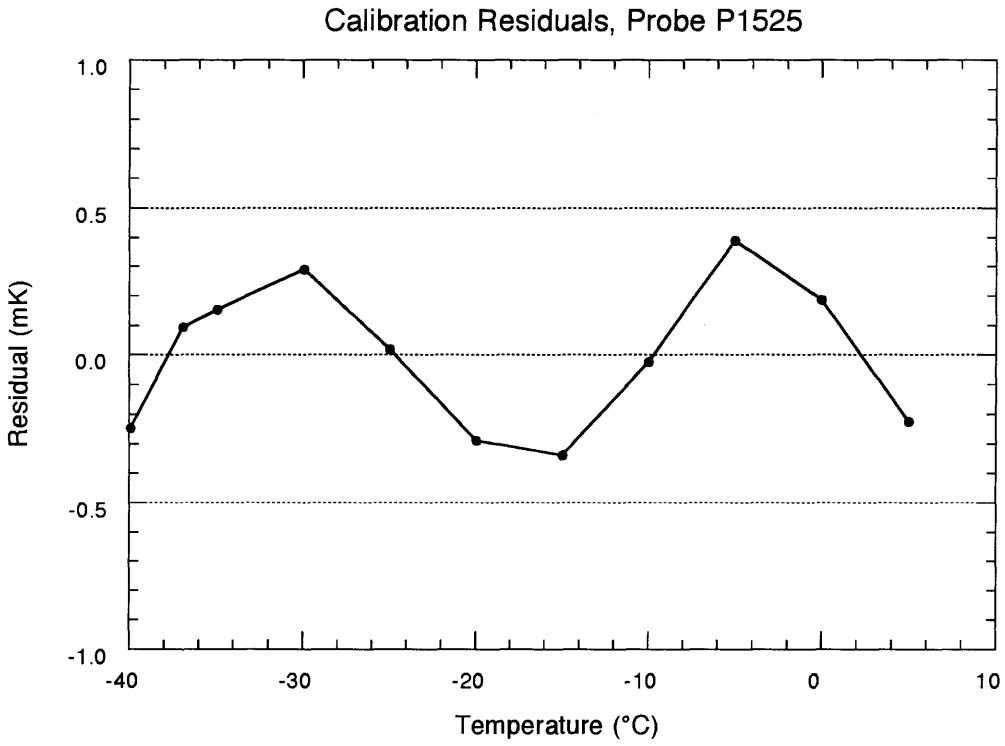

Figure 5: The difference between the measured calibration data for probe P1525 and the calibration function determined using least squares. Based on the residuals, the uncertainty in the calibration function is 0.27 mK at the approximate temperature of the 1992 GISP2 temperature log.

much faster than that of the temperature sensor (15 s), allowing the circuit to detect any resistance change experienced by the probe. The temperature error ϵ_c due to the cable's capacitance was less than 5.4 μK. A system check with the probe sitting at 305 m for about 35 minutes validated the stability of the electronics at the 0.14 mK level (Fig. 10).

Table 1. Factors affecting the uncertainty of the May 1992 GISP2 temperature measurements.

Source	Magnitude
system sensitivity, ΔT	0.14 mK
inter-conductor leakage error, ϵ_l	< 0.23 mK
self-heating effect, ϵ_h	0.23 mK
capacitance effect, ϵ_c	< 5.4 μK
probe calibration error	0.27 mK
multimeter calibration error	0.15 mK
slip-ring noise	1.5 mK

The May 1992 log was obtained in the system's continuous mode, using a logging speed of ~ 7.4 cm s^{-1}. One measurement was acquired every 2.0 s, providing a sample spacing of ~ 15 cm. Given the response time of 15 s for the thermistor probe, the sampling rate was high enough to prevent any aliasing of the temperature signal. A close inspection of the data (Fig. 6) reveals the presence of random noise at the ± 1.5 mK level. This noise dominates the measured signal at all frequencies above 0.004 Hz, corresponding to wavelengths (dz) less than 18.5 m with a logging speed of 7.4 cm s^{-1}. Although a small portion (0.14 mK) of the random noise can be attributed to the finite resolution of the multimeter, the bulk of it was due to the slip-ring assembly which provides electrical continuity between the multimeter and the logging cable (mounted on a rotating drum). Slip-ring noise is inherent to some degree in all continuous temperature logs. With our depth measuring system, various factors can cause errors in the recorded location of the temperature probe while logging. These factors include: cable slippage on the depth measurement pulley, cable stretch, thermal expansion or contraction of the cable, or cable hangups in the hole. Despite these potential problems, the total hole depth recorded at the end of the May 1992 log was 1510.56–1510.59 m, in close agreement with the depth determined by the Polar Ice Coring Office using the kevlar drilling cable and with the depth found by adding up the lengths of the ice cores that had been extracted from the borehole.

We processed the GISP2 data in the following way: 1) The measured resistances were first corrected for the self-heating effect, i.e. they were changed to what would have been recorded if the multimeter's excitation current had been zero. Due to the uncertainty in the power dissipation constant, the correction is not perfect. We estimate up to 0.05 mK of self-heating may still be present in the data. 2) The corrected resistances were then converted to temperature using the calibration constants for probe P1525 in Equation 5. Again, probe calibration errors lead to an 0.27 mK uncertainty in the temperatures derived from the calibration function. 3) The high-frequency slip-ring noise was effectively filtered

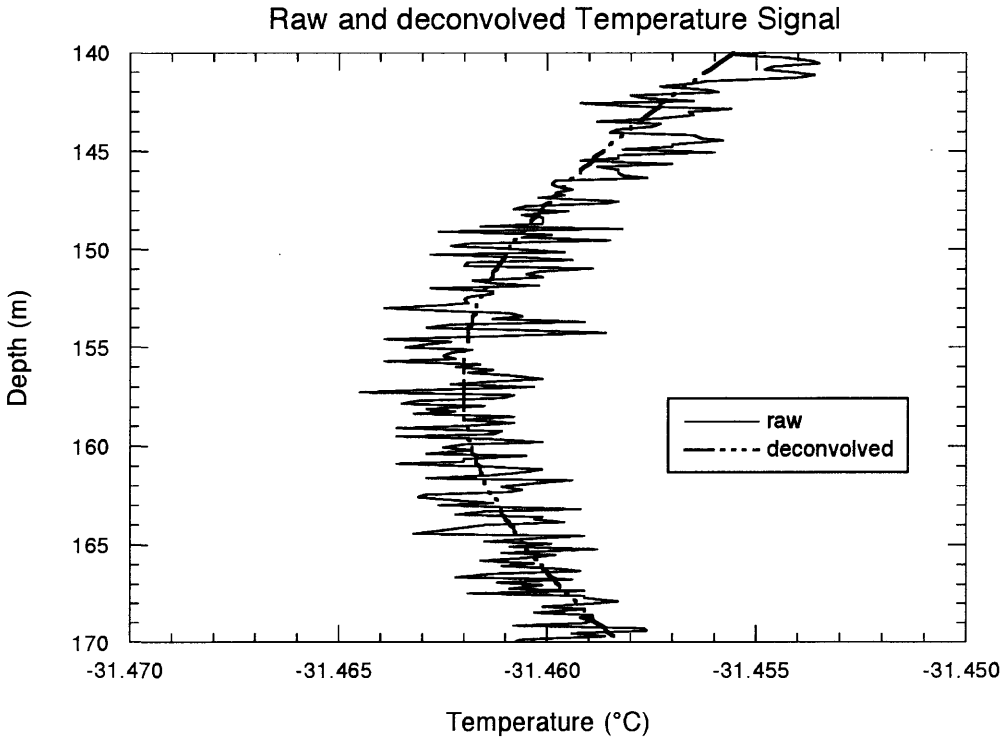

Figure 6: Raw temperature measurements (solid line) from 140 to 170 m showing the effects of the slip-ring noise (standard error 1.5 mK). This noise is reduced to about 0.25 mK through optimal filtering. The deconvolved signal obtained from the filtered data is show by the dashed line; deconvolution is required to account for the relatively slow response time (15 s) of the moving temperature sensor.

in the frequency domain using optimal (Wiener) filtering (*Saltus and Clow*, 1994). This filtering reduced the standard error of the random noise to about 0.25 mK. 4) Finally, the filtered data were deconvolved using serial division to obtain the actual borehole temperatures from the data acquired with the moving sensor (*Saltus and Clow*, 1994). The accuracy of the serial division is estimated to be 0.6 mK for the May 1992 log (this includes the effects of the random noise). After the above processing steps, we estimate the precision of the May 1992 temperature measurements to be 0.7 mK while the accuracy is 4.5 mK.

Table 2. Sources of uncertainty in the GISP2 temperature measurements after data processing.

Source	Magnitude
inter-conductor leakage error	< 0.23 mK
self-heating error	~ 0.05 mK
probe calibration error	0.27 mK
multimeter calibration error	0.15 mK
deconvolution accuracy	0.60 mK

Figures 7 and 8 show the resulting temperature profile and temperature gradient in the GISP2 borehole during May, 1992. No data were acquired in the air-filled portion of the hole so the log begins at about 83 m. Coming up from the bottom of the record, the warming beginning at 1500 m depth is due to the onset of the Holocene period, the cooling starting at 800 m is associated with cooler temperatures following the Holocene Optimum, and the warming above 150 m post-dates the Little Ice Age.

Fluid Convection

Thus far we have only discussed instrumental uncertainties. For large diameter boreholes such as GISP2 (18 cm), buoyancy forces are often sufficiently great that the fluid filling the borehole freely convects. When this occurs, temperature fluctuations associated with the convective flow can be an additional source of thermal noise. This is a pervasive problem in the 33-cm diameter boreholes we periodically log in northern Alaska (e.g., *Lachenbruch et al.*, 1988; *Lachenbruch and Marshall*, 1986; *Lachenbruch et al.*, 1982). In these holes, the convection is fully turbulent, producing random temperature fluctuations of 10–50 mK. In Greenland, fluid convection has been inferred to occur within the 13-cm diameter Dye 3 borehole, at least at depths below 1600 m (*Hansen and Gundestrup*, 1988). Based on the discussion of Hansen and Gundestrup, the fluid flow in Dye 3 appears to be laminar and is expressed by temperature discontinuities of ≈ 100 mK at discrete depths; the cells are about 20 m high.

Fluid convection should occur whenever the local temperature gradient exceeds the adiabatic lapse rate plus the critical potential-temperature gradient,

$$(\frac{\partial T}{\partial z}) > \frac{g\alpha T}{C_p} + (\frac{\partial \theta}{\partial z})_{crit}, \tag{6}$$

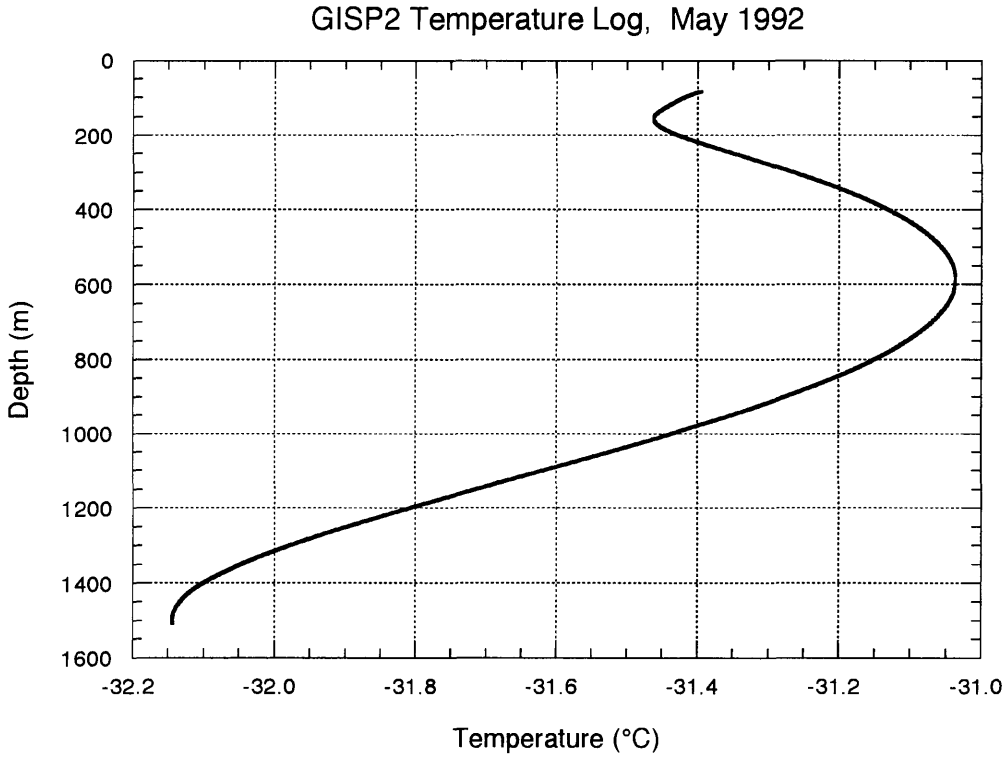

Figure 7: The processed May 1992 GISP2 temperature log. The precision of this log is 0.7 mK and the accuracy is 4.5 mK.

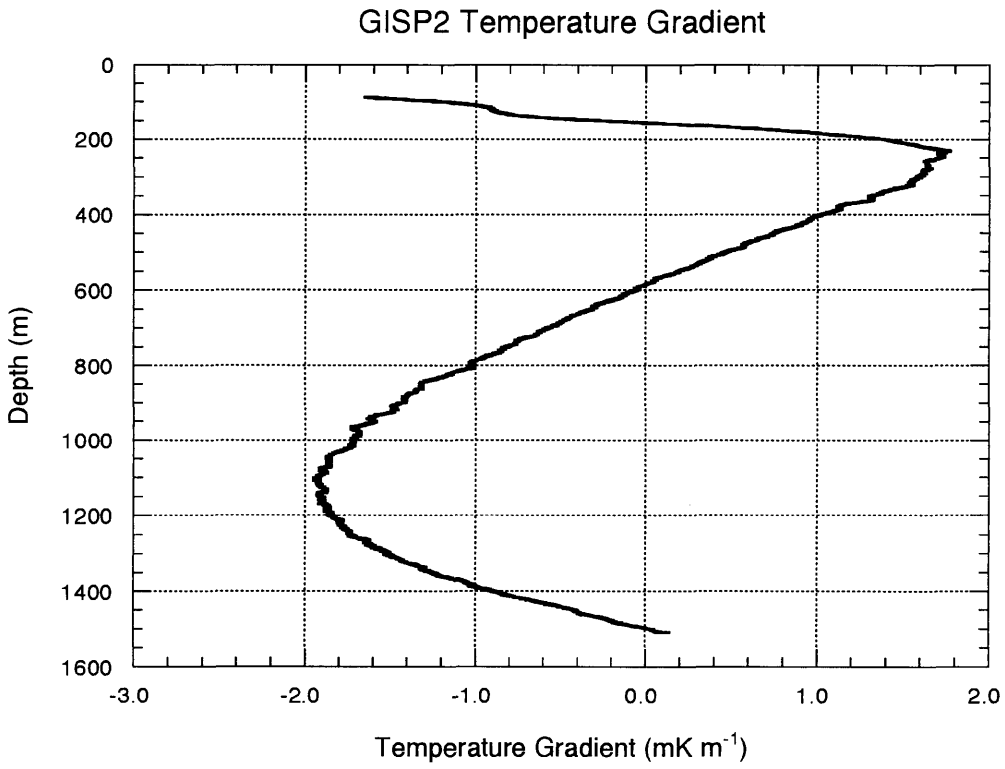

Figure 8: Temperature gradients in the GISP2 borehole during May 1992.

where α is the coefficient of thermal expansion for the borehole fluid, C_p is the specific heat, g is the gravitational acceleration, and T is temperature expressed in Kelvin. The critical potential-temperature gradient,

$$(\frac{\partial\theta}{\partial z})_{crit} = \frac{\nu\kappa}{\alpha g r^4}(Ra_c\gamma^4), \tag{7}$$

accounts for the effects of viscous drag within the fluid and the boundary conditions at the wall of the borehole; ν is the kinematic viscosity, κ is the thermal diffusivity, r is the borehole radius, $\gamma = (r/L)$ is the aspect ratio for convective cells of length (height) L, and Ra_c is the critical Rayleigh number (which is a function of γ). Using linear stability analysis, *Charlson and Sani* (1970, 1971) have determined the Rayleigh numbers of the most unstable convective modes for aspect ratios between 0 and 8 when the side walls could be regarded as either a perfect thermal insulator or a perfect conductor. A no-slip condition was imposed on the side walls. They found that $(Ra_c\gamma^4)$ approaches a minimum as $\gamma \rightarrow 0$ and that the most unstable mode is a single antisymmetric cell with an aspect ratio less than 0.1; this is consistent with experimental observations. The minimum $(Ra_c\gamma^4)$-values were found to be about 71 in the limit of perfectly insulating side walls and 220 for perfectly conducting walls.

The deep hole at GISP2 is primarily filled with n-butyl acetate and has a nominal diameter of 18.1 cm. Based on data supplied by Union Carbide, butyl acetate has the following properties at −30°C: $\alpha = 0.00109$ K^{-1}, $\nu = 1.76$ x 10^{-6} m^2 s^{-1}, $\kappa = 8.60$ x 10^{-8} m^2 s^{-1}, and the specific heat is estimated to be 1850 J kg^{-1} K^{-1}. Given these values, the adiabatic lapse rate for the GISP2 borehole fluid is 1.41 mK m^{-1} while the critical potential-temperature gradient is much smaller, 0.015–0.046 mK m^{-1}, depending on the thermal conductivity of the walls. Thus, the scale of the system is large enough that the onset of convection is determined predominantly by the adiabatic lapse rate. Convection is expected to occur at all depths where the local temperature gradient exceeds 1.46 mK m^{-1}. The *form* of the convective flow depends on the ratio of the Rayleigh number Ra to the critical Rayleigh number Ra_c associated with the most unstable mode. Figure 9 shows the (Ra/Ra_c) ratio calculated for GISP2 as a function of the aspect ratio and the local temperature gradient. Sufficient buoyant energy is available to drive cells of aspect ratio γ whenever (Ra/Ra_c) is greater than 1. Note that cells with aspect ratios less than ≈ 0.2 all have about the same energy requirements. For temperature gradients of about 1.6 mK m^{-1}, the predicted flow within the GISP2 borehole is very organized and steady in time (see *Tritton*, 1988). For gradients of 3–5 mK m^{-1}, the predicted flow is still spatially organized but oscillatory in time, while the transition to fully turbulent flow is expected to occur at about 10 mK m^{-1}.

Within the upper 1510 m of the borehole accessible during May 1992, the observed temperature gradient (Fig. 8) slightly exceeds the convective onset value in the 210–330 m depth range. In this zone, the upper limit of the (Ra/Ra_c) ratio is probably about 8, suggesting well-organized steady convection cells with a minimum height of 14 cm. Cell heights in the range 1 to tens of meters are favored energetically. In an effort to detect convection within this zone, we monitored temperatures at a depth of 305 m for a period of 30 minutes (Fig. 10). We failed to detect any temperature fluctuations during this test, suggesting the following possibilities: a) the convective flow is so steady that the convective

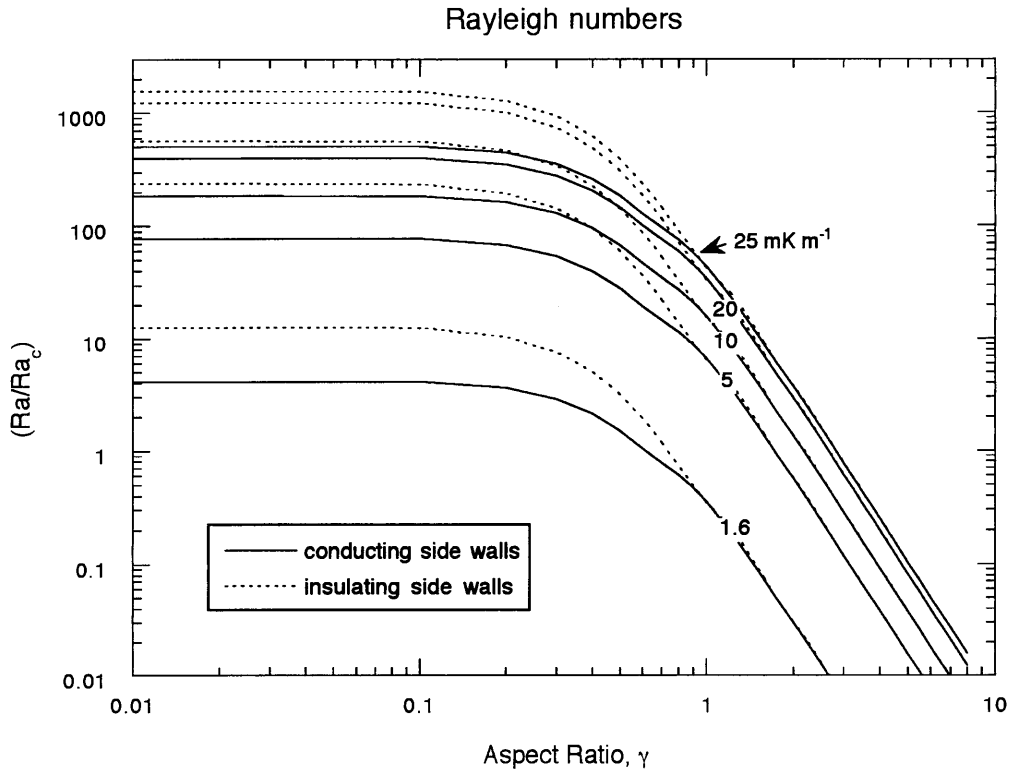

Figure 9: Ratio of the Rayleigh number Ra to the critical Rayleigh number Ra_c, calculated for the GISP2 borehole.

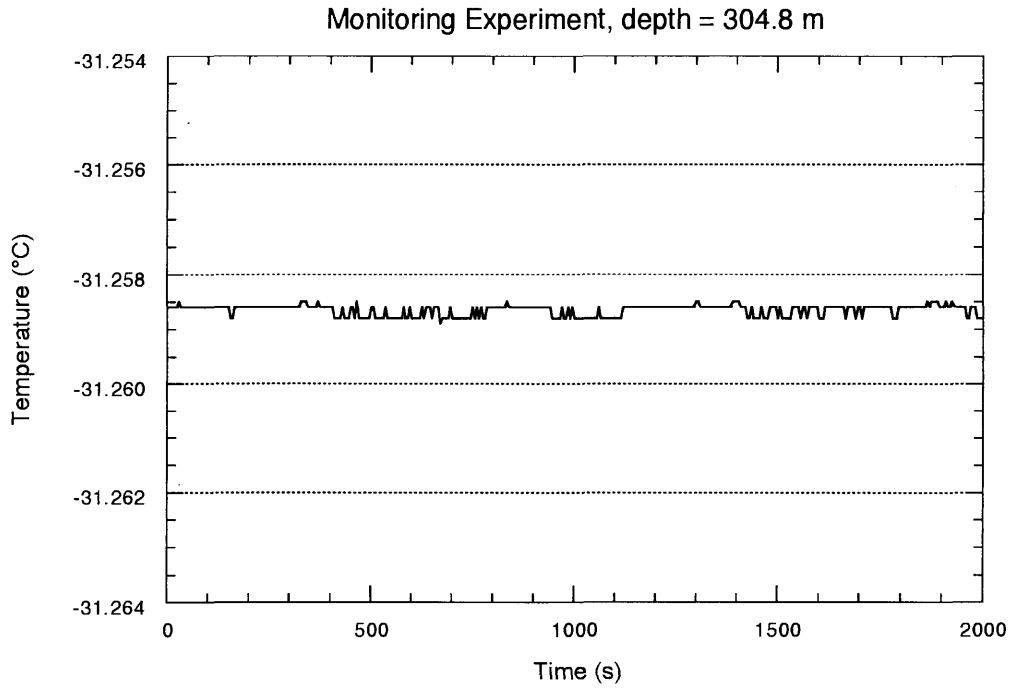

Figure 10: Temperatures monitored at 304.8 m in the GISP2 borehole show no evidence of fluid convection. The monitoring experiment also demonstrates the electronic stability of the logging system. The small changes are at the threshold of the system's sensitivity, 0.14 mK.

temperature fluctuations are less than the sensitivity of the logging system, 0.14 mK, b) the unsteady component of the flow has a period much greater than 30 minutes, or c) convection does not occur at all in the vicinity of 305 m. Because the physical properties of butyl acetate are only approximately known at the conditions existing in the GISP2 borehole, option (c) is a distinct possibility.

Drilling continued to deepen the GISP2 borehole following our May, 1992 temperature measurements until bedrock was eventually encountered at 3054 m on July 1, 1993. Subsequent temperature measurements by GDC show a progressive increase in the temperature gradient from 0.4 mK m^{-1} at 1510 m to 25 mK m^{-1} at the bed of the ice sheet. Rapid temperature fluctuations associated with convective flow were observed at all depths where the gradient exceeds the convective onset value.

Drilling Disturbance

Temperatures in the ice surrounding the deep borehole were disturbed by four processes during the drilling: 1) The drill motor located on the downhole end of the drilling cable consumed about 1.6 kW of electrical power while it was running. This power was converted to heat and transferred to the drilling fluid. Because there was little mixing of the drilling fluid in the borehole as the core tubes were repeatedly brought to the surface

(Walt Hancock, personal communication), the heat from the drilling motor can be treated as a point source. 2) About 600 W were lost in the drilling cable due to resistive heating while the drill motor was operating. This heat was then radiated along the entire length of the cable. 3) As the hole was deepened, the entire fluid column in the borehole moved downwards, advecting heat with it. 4) Drilling fluid was periodically added to the hole as it was deepened in order to maintain the fluid level at about 90 m (near the ice/firn transition). The added fluid is estimated to have been 5–25 K warmer, depending on time of year, than the ice surrounding the upper 1510 m of the borehole (Dave Giles, personal communication). Of these effects, the first and the last were by far the largest; the other two are discussed for completeness.

The transfer of excess heat from the drilling fluid at any depth z to the surrounding ice proceeded fairly rapidly. This can be demonstrated by considering the following experiment: suppose a parcel of borehole fluid and the surrounding ice are initially in thermal equilibrium. Instantaneously raise the fluid temperature by an amount ΔT_0. The thermal disturbance at time t following this heating event can be approximated by

$$\Delta T(r,t) = \frac{4\Delta T_0 K_1 K_2 \kappa_2}{\pi^2 a} \int_0^\infty e^{-\kappa_1 u^2 t} \frac{J_0(ur)J_1(ua)du}{u^2[\phi^2(u)+\psi^2(u)]}, \quad (r \le a), \tag{8}$$

$$\Delta T(r,t) = \frac{2\Delta T_0 K_1 \kappa_2^{1/2}}{\pi} \int_0^\infty e^{-\kappa_1 u^2 t} \frac{J_1(ua)[J_0(\kappa ur)\phi(u) - Y_0(\kappa ur)\psi(u)]du}{u[\phi^2(u)+\psi^2(u)]}, (r > a), \tag{9}$$

where

$$\psi(u) = K_1 \kappa_2^{1/2} J_1(au)J_0(\kappa au) - K_2 \kappa_1^{1/2} J_0(au)J_1(\kappa au) \tag{10}$$

$$\phi(u) = K_1 \kappa_2^{1/2} J_1(au)Y_0(\kappa au) - K_2 \kappa_1^{1/2} J_0(au)Y_1(\kappa au) \tag{11}$$

and J_0, Y_0, J_1, and Y_1 are the zero- and first-order Bessel functions (*Carslaw and Jaeger*, section 13.8). K_1 and κ_1 are the thermal conductivity (0.148 W m^{-1} K^{-1}) and thermal diffusivity of the borehole fluid (butyl acetate), respectively, while K_2 and κ_2 are the analogous properties for ice; $\kappa = \sqrt{(\kappa_1/\kappa_2)}$. Figure 11 shows the evolution of the drilling disturbance in the vicinity of the borehole. Over 90% of the excess heat is transferred from the borehole fluid to the surrounding ice within 16 hours of the heating event.

The assumptions inherent in Equations 8 and 9 make it difficult to apply to the GISP2 disturbance problem which involves multiple heat sources of varying durations. An easier approach is to use the relationship developed by *Lachenbruch and Brewer* (1959) to describe the thermal disturbance caused by a heat source of duration S,

$$\Delta T(t) = \frac{Q}{4\pi s K_2} \ln\left(\frac{t}{t-S}\right), \tag{12}$$

that is assumed to be uniform in time. Here, Q is to total heat released per unit length of borehole during the heating event and time t begins at the onset of heating. The validity of Equation 12 is limited to normalized times (t/S) greater than about 5.

During the 1990 field season, drilling began at a depth of 90 m on 6 July and finished at 335 m on 25 August. During 1991, drilling advanced from 335 m on 4 June to 1510 m on 28 August. It took, on average, 2508 s to drill a 5.9 m section of core at GISP2. Given a power consumption of 1.6 kW, 4.01 MJ were used by the motor to drill a 5.9 m core. The

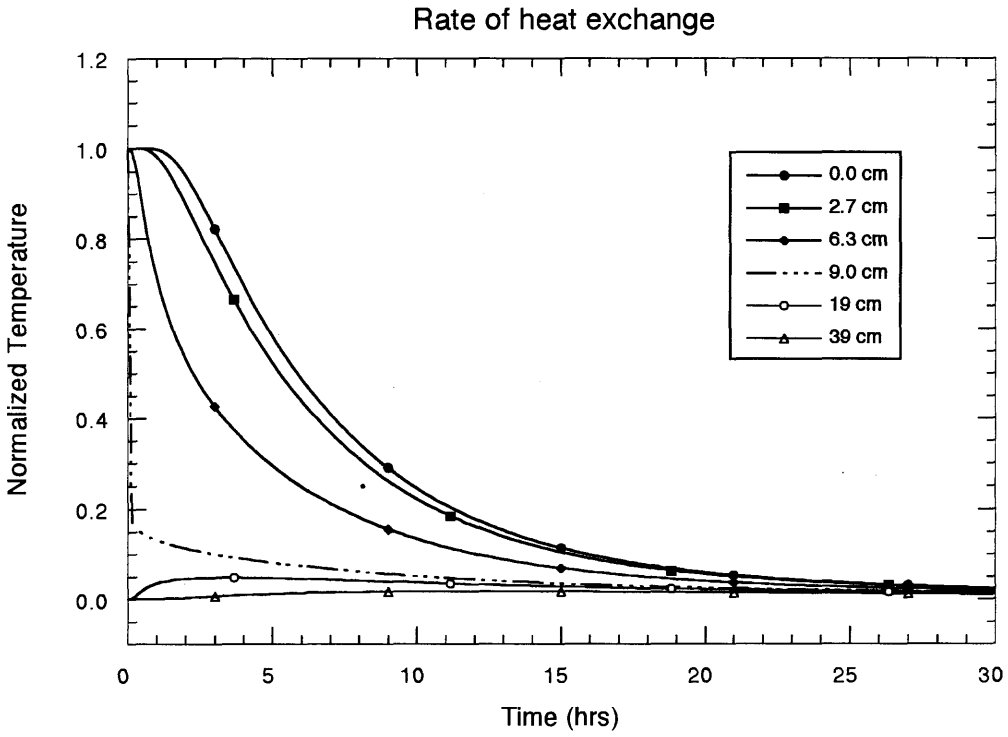

Figure 11: Normalized temperatures $[\Delta T(r,t)/\Delta T_o]$ inside and outside a borehole of radius 9 cm. Temperatures inside the borehole were initially at $T = \Delta T_o$ while those outside the hole were at zero.

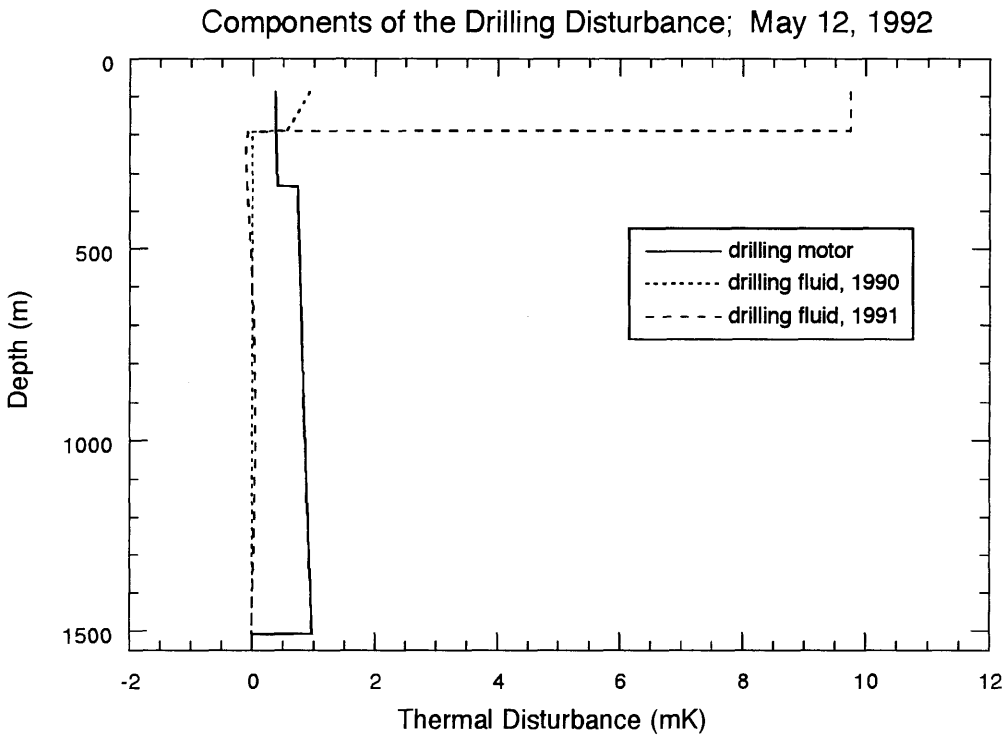

Figure 12: Drilling disturbance remaining at the time of the 1992 temperature log due to the drilling motor, the addition of relatively warm fluid to the top of the borehole (90 m $< z <$ 190 m), and the advection of heat by the descending fluid column ($z >$ 190 m). The dominant disturbance was caused by the warm fluid periodically injected to the hole to maintain the fluid level. The jog in the drill-motor disturbance at 335 m is because depths between 90 and 335 m were drilled during 1990 while those in the 335-1510 m depth range were drilled during 1991.

total heat released by the advancing motor was then $Q_m = 0.68$ MJ m^{-1}. Figure 12 shows the thermal disturbance at various depths due to the drill motor, based on Equation 12. By the time of the 12 May, 1992 temperature log, the drill-motor disturbance is predicted to have dissipated to 0.4–1.0 mK.

The thermal disturbance associated with the drilling cable was quite small. With 600 W of electrical power being lost in a cable about 3500 m long, the magnitude of this heat source was only 0.171 W m^{-1}. This only occurred when the drill motor was actually running. When averaged over the entire drilling season, the cable heat source was 4.12 mW m^{-1} during the summer of 1990 and 11.63 mW m^{-1} during 1991. The duration of the cable heating at any depth depended on how long the motor had been drilling below that depth. Thus, the maximum cable disturbance was experienced at shallow depths. Between 90 and 335 m, the total heat radiated by the cable during the 1991 drilling season was $Q_c = 0.085$ MJ m^{-1}. By 12 May, 1992, the associated thermal disturbance is predicted to have decayed to only 0.11 mK (Eq. 12). Similarly, the disturbance due to cable heating during the 1990 drilling season would have decayed to less than 0.01 mK

by the time of the 1992 temperature log.

As the borehole was deepened, the fluid column in the hole moved downwards, advecting heat with it. We can approximate the advection process by assuming the fluid column moved downhole instantaneously at the end of each drilling day by an amount Δz, which was equal to the mean drilling rate for the season (4.90 m day^{-1} during 1990 and 13.82 m day^{-1} during 1991). Given this assumption, the resulting mean heat flux through the borehole wall would have been

$$q_f = \frac{(\rho C_p)_f (T_f - T_i)}{\Delta t} (\frac{a}{2}), \tag{13}$$

where $(\rho C_p)_f$ is the volume specific heat of n-butyl acetate (1.72 MJ m^{-3} K^{-1}), T_f is the temperature of a parcel of butyl initially at depth $z - \Delta z$, T_i is the equilibrium ice temperature at z, and Δt is the amount of time required to transfer the bulk of the heat through the borehole wall. As demonstrated earlier, Δt is of order 16 hours so the fluid temperatures would have approached the local ice temperature before the column is assumed to move again at the end of the next drilling day. Because the drilling rate is assumed to be uniform throughout each drilling season, the mean-daily flux q_f at any depth z remains fixed throughout the drilling season. Summing up over an entire drilling season, the total heat transferred between the fluid and the surrounding ice at depth z is then

$$Q_f = \frac{\pi a^2 S (\rho C_p)_f (T_f - T_i)}{\Delta t}, \tag{14}$$

where S is the number of days the hole was drilled at depths greater than z. As of 12 May, 1992, the maximum fluid disturbance (Fig. 12) occurred in the 210–300 m depth range where the temperature gradient is relatively steep. For the 1991 drilling season, the flux q_f at these depths was about -20 mW m^{-2} and the total heat transfer for the season was $Q_f \approx -0.083$ MJ m^{-1}. The resulting thermal disturbance is predicted to have decayed to -0.10 mK by the time of the 1992 temperature log (Eq. 12).

The final drilling-disturbance process we consider involves the periodic addition of fluid to the borehole to maintain the fluid level near 90 m. Of all the processes discussed, this is the most uncertain because: 1) no record was kept of the fluid temperature prior to injecting it into the hole, and 2) little is known concerning the extent to which the injected fluid mixed with the fluid already in the borehole. Dave Giles (Polar Ice Coring Office) estimates the injected fluid may have been 5–25 K warmer, depending on time of year, than the ambient ice temperature surrounding the upper 1510 m of the borehole. To estimate the magnitude of this disturbance, we will assume: 1) the injected fluid was 15 K warmer than the section of borehole into which it was injected, 2) the new fluid rapidly mixed with the old fluid over the 90–190 m depth range, and 3) fluid injection occurred at the end of each drilling day. The mean-daily flux q_f through the borehole wall in the 90–190 m depth range can then be found by multiplying the r.h.s. of Eq. 13 by (Δz/100 m) where 100 m is the mixing length. Similarly, the total heat Q_f transferred from the injected fluid to the ice (in the 90–190 m zone) is found by multiplying the r.h.s. of Eq. 14 by (Δz/100 m). For the 1991 drilling season, the flux q_f due to fluid injection was roughly 1.9 W m^{-2} (90 m $< z <$190 m) and the associated total heat transfer Q_f was 7.8 MJ m^{-1}. From Eq. 12, the associated thermal disturbance was about 9.8 mK at the time of the 1992 temperature log (Fig. 12).

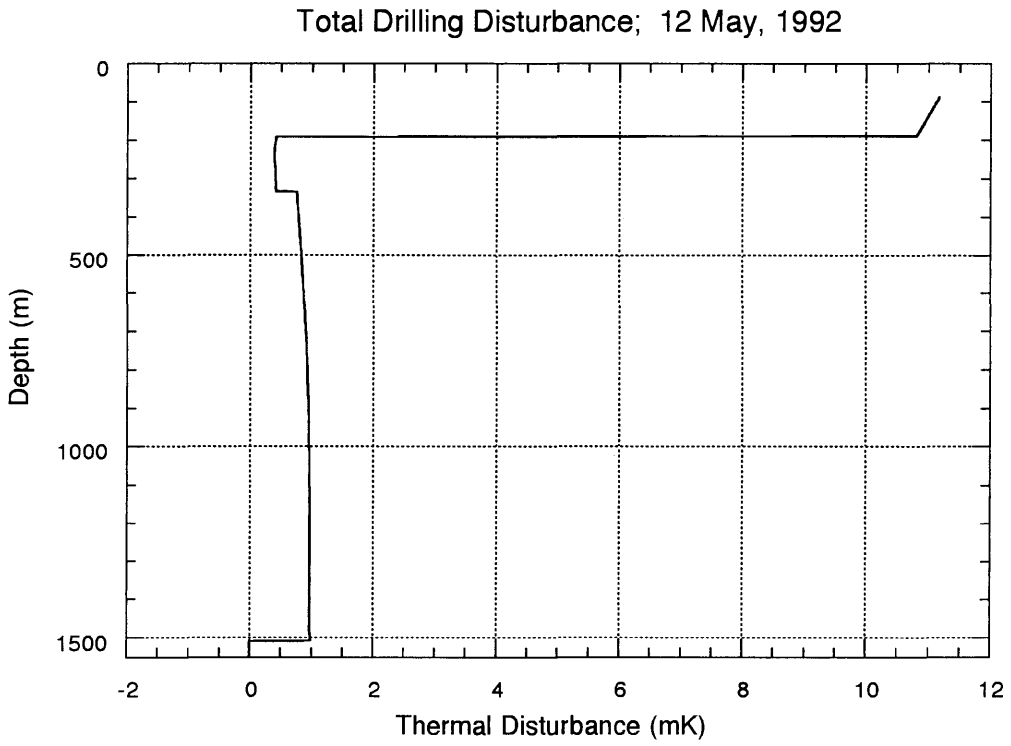

Figure 13: Predicted drilling disturbance due to all processes at the time of the 1992 temperature log.

The total drilling disturbance at the time of the 1992 temperature log is shown in Figure 13. For the bulk of the borehole, the disturbance is predicted to have decayed to about the 1 mK level. However, the upper section of the borehole is predicted to have still been severely disturbed. Again, the magnitude and extent of the upper hole disturbance are poorly known due to uncertainties in injected fluid's temperature and the extent to which it mixed with the fluid already in the hole. Thus, the details of the upper hole disturbance should be viewed with caution. Analysis of several temperature logs, acquired annually, will greatly improve our understanding of the drilling disturbance in the GISP2 borehole.

Concluding Remarks

It is currently possible to make borehole temperature measurements within ice sheets with a precision better than 1 mK. To achieve this, the interaction of the measuring circuit and the probe must be carefully considered in order to optimize the system's sensitivity and to minimize inter-conductor leakage effects and self-heating effects. Calibration procedures must also be carefully considered. The "slip-ring" noise produced during continuous logs can be substantially removed through optimal filtering. Although the deconvolution process used to remove the effect of a temperature probe's relatively slow response time does amplify the random noise, it is still possible to attain a precision of better than 1 mK

in the processed data. The availability of data with this precision should allow a marked improvement in the surface-temperature histories reconstructed from borehole temperature measurements. In addition, it may allow the direct detection of shear heating near the bed of an ice sheet.

The new logging system was used to obtain a temperature log in the GISP2 borehole before drilling operations began for the 1992 field season. The processed log, consisting of about 10,000 measurements, has a precision of 0.7 mK and an accuracy of 4.5 mK. Our analysis indicates that no fluid convection should occur in the upper 1510 m of the GISP2 borehole available during May 1992, except for a narrow zone between 210 and 330 m which is predicted to be slightly unstable. However, a temperature monitoring experiment with a sensitivity of 0.14 mK conducted at 305 m, failed to detect any evidence of fluid convection. Nevertheless, the borehole fluid is predicted to be turbulently convecting in the lower portion of the now completed borehole. Although the hole had been idle for 8.5 months at the time of the May 1992 temperature log, the thermal disturbance due to the previous year's drilling activities is predicted to have still been of order 10 mK in the upper couple hundred meters of the borehole. Analysis of several temperature logs, acquired annually, will be required to improve our understanding of the magnitude and extent of the drilling disturbance. If the predicted disturbance as of May 1992 is approximately correct, it will take an additional ~ 7 years for the drilling disturbance to dissipate to the 1 mK level.

Acknowledgments. This work was supported by the USGS Global Change and Climate History Program and the GISP2 Science Management Office. We thank Jack Kennelly and Walt Wendt who built much of the equipment; Jim Tatgenhorst, Mark Wumkes, and Dave Giles, all of whom provided invaluable assistance in the field; Michael Morrison for his encouragement; and finally the 109^{th} Air National Guard.

References

Beck, A.E., and N. Balling. 1988. Determination of virgin rock temperatures, *in* Haenel, R., Rybach, L., and L. Segena, (eds), *Handbook of Terrestrial Heat-Flow Determination*, 59–85.

Bevington, P.R. 1969. *Data Reduction and Error Analysis for the Physical Sciences*, McGraw-Hill, 336 pp.

Carslaw, H.S. and J.C. Jaeger. 1959. *Conduction of Heat in Solids*, Clarendon Press, 2nd edition, 510 pp.

Charlson, G.S. and R.L. Sani. 1970. Thermoconvective instability in a bounded cylindrical fluid layer, *Int. J. Heat Mass Transfer*, **13**, 1479–1496.

Charlson, G.S. and R.L. Sani. 1971. On thermoconvective instability in a bounded cylindrical fluid layer, *Int. J. Heat Mass Transfer*, **14**, 2157–2160.

Clow, G.D. 1992. The extent of temporal smearing in surface-temperature histories derived from borehole temperature measurements, *Palaeogeography, Palaeoclimatology, Palaeoecology*, **98**, 81-86.

Hansen, B.L. and N.S. Gundestrup. 1988. Resurvey of bore hole at Dye 3, South Greenland, *J. Glaciol.*, **34**, 178–182.

Lachenbruch, A.H. and M.C. Brewer, 1959, Dissipation of the temperature effect of drilling a well in Arctic Alaska, *U.S. Geological Survey Bulletin 1083-C*, 73–109.

Lachenbruch, A.H. and B.V. Marshall, 1986, Changing climate; geothermal evidence from permafrost in the Alaskan Arctic, *Science*, **234**, 689–696.

Lachenbruch, A.H., Sass, J.H., Marshall, B.V. and T.H. Moses, Jr., 1982, Permafrost, heat flow, and the geothermal regime at Prudhoe Bay, Alaska, *J. Geophys. Res.*, **87**, 9301–9316.

Lachenbruch, A.H., Sass, J.H., Lawver, L.A., Brewer, M.C., Marshall, B.V., Munroe, R.J., Kenelly, J.P., Jr., Galanis, S.P., Jr. and T.H. Moses, Jr., 1988, Temperature and depth of permafrost on the Arctic slope of Alaska, *in* Geology and exploration of the National Petroleum Reserve in Alaska, 1974 to 1982, Gryc, George, *U.S. Geological Survey Professional Paper P 1399*, 645–656.

Press, W.H., Flannery, B.P., Teukolsky, S.A., and W.T. Vetterling, 1992. *Numerical Recipes in FORTRAN: The Art of Scientific Computing*, Cambridge University Press, 963 p.

Saltus, R.W. and G.D. Clow. 1994. Deconvolution of continuous borehole temperature logs: Example from the Greenland GISP2 icecore hole, *U.S. Geological Survey Open-File Report 94-254*, 47 pp.

Sass, J.H., Lachenbruch, A.H., Munroe, R.J., Greene, G.W., and T.H. Moses, Jr. 1971. Heat flow in the western United States, *Journal of Geophysical Research*, **15**, 6376–6413.

Steinhart, J.S. and S.R. Hart. 1968. Calibration curves for thermistors, *Deep-Sea Research*, **15**, 497-503.

Tritton, D.J. 1988. *Physical Fluid Dynamics*, 2nd edition, Clarendon Press, 519 pp.